Atmospheric
Measurement
Techniques

A simple calculation algorithm to separate high-resolution CH₄ flux measurements into ebullition- and diffusion-derived components

Mathias Hoffmann[1], **Maximilian Schulz-Hanke**[2], **Juana Garcia Alba**[1], **Nicole Jurisch**[2], **Ulrike Hagemann**[2], **Torsten Sachs**[3], **Michael Sommer**[1,4], **and Jürgen Augustin**[2]

[1]Institute of Soil Landscape Research, Leibniz Centre for Agricultural Landscape Research (ZALF) e.V.,
Eberswalder Str. 84, 15374 Müncheberg, Germany
[2]Institute of Landscape Biogeochemistry, Leibniz Centre for Agricultural Landscape Research (ZALF) e.V.,
Eberswalder Str. 84, 15374 Müncheberg, Germany
[3]GFZ German Research Centre for Geosciences, Telegrafenberg, 14473 Potsdam, Germany
[4]Institute of Earth and Environmental Sciences, University of Potsdam, Karl-Liebknecht-Str. 24–25,
14476 Potsdam, Germany

Correspondence to: Mathias Hoffmann (mathias.hoffmann@zalf.de)

Abstract. Processes driving the production, transformation and transport of methane (CH₄) in wetland ecosystems are highly complex. We present a simple calculation algorithm to separate open-water CH₄ fluxes measured with automatic chambers into diffusion- and ebullition-derived components. This helps to reveal underlying dynamics, to identify potential environmental drivers and, thus, to calculate reliable CH₄ emission estimates. The flux separation is based on identification of ebullition-related sudden concentration changes during single measurements. Therefore, a variable ebullition filter is applied, using the lower and upper quartile and the interquartile range (IQR). Automation of data processing is achieved by using an established R script, adjusted for the purpose of CH₄ flux calculation. The algorithm was validated by performing a laboratory experiment and tested using flux measurement data (July to September 2013) from a former fen grassland site, which converted into a shallow lake as a result of rewetting. Ebullition and diffusion contributed equally (46 and 55 %) to total CH₄ emissions, which is comparable to ratios given in the literature. Moreover, the separation algorithm revealed a concealed shift in the diurnal trend of diffusive fluxes throughout the measurement period. The water temperature gradient was identified as one of the major drivers of diffusive CH₄ emissions, whereas no significant driver was found in the case of erratic CH₄ ebullition events.

1 Introduction

Wetlands and freshwaters are among the main sources for methane (CH₄), which is one of the major greenhouse gases (Dengel et al., 2013; Bastviken et al., 2011; IPCC, 2013). In wetland ecosystems, CH₄ is released via three main pathways: (i) diffusion (including "storage flux", in terms of rapid diffusive release from methane stored in the water column), (ii) ebullition and (iii) plant-mediated transport (e.g. Goodrich et al., 2011; Bastviken et al., 2004; Van der Nat and Middelburg, 2000; Whiting and Chanton, 1996). The magnitude of CH₄ released via the different pathways is subject to variable environmental drivers and conditions such as water level, atmospheric pressure, temperature gradients, wind velocity and the presence of macrophytes (Lai et al., 2012; Tokida et al., 2007; Chanton and Whiting, 1995). As particularly ebullition varies in time and space (Maeck et al., 2014; Walter et al., 2006), total CH₄ emissions feature an extremely high spatial and temporal variability (Koch et al., 2014; Repo et al., 2007; Bastviken et al., 2004). Hence, attempts to model CH₄ emissions based on individual environmental drivers are highly complex. To identify relevant environmental drivers of CH₄ emissions, the separation of measured CH₄ emissions into the individual pathway-associated components is crucial (Bastviken et al., 2011, 2004). Moreover, the understanding of the complex processes determining the temporal and spa-

tial patterns of CH$_4$ emissions is a prerequisite for upscaling field-measured CH$_4$ emissions to the landscape or regional scale, and thus for adequately quantifying the contribution of wetland CH$_4$ emissions to global greenhouse gas (GHG) budgets (Walter et al., 2015; Koebsch et al., 2015; Lai et al., 2012; Limpens et al., 2008).

However, field studies measuring CH$_4$ release above shallow aquatic environments or flooded peatlands generally measure total CH$_4$ emissions as a mixed signal of individual CH$_4$ emission components, released via all possible pathways (i.e. diffusion, ebullition and plant-mediated transport). Studies separately measuring temporal and spatial patterns of CH$_4$ emissions resulting only from either ebullition or diffusion are rare. Measurements of CH$_4$ ebullition can be performed using manual or automatic gas traps, as well as optical and hydro-acoustic methods (Wik et al., 2013, 2011; Maeck et al., 2014; Walter et al., 2008; Ostrovsky et al., 2008; Huttunen et al., 2001; Chanton and Whiting, 1995), often requiring considerable instrumentation within the studied system. Diffusive CH$_4$ fluxes are commonly either derived indirectly as the difference between total CH$_4$ emissions and measured ebullition, or directly obtained based on the use of bubble shields or gradient measurements of CH$_4$ concentration differences (DelSontro et al., 2011; Bastviken et al., 2010, 2004). A graphical method to separate diffusion, steady ebullition and episodic ebullition fluxes from the total CH$_4$ flux was presented by Yu et al. (2014), using a flow-through chamber system. However, performed at the laboratory scale for a peat monolith, measurement results as well as the applied method were lacking direct field applicability. A first simple mathematical approach for field measurements to separate ebullition from the sum of diffusion and plant-mediated transport was introduced by Miller and Oremland (1988), who used low-resolution static chamber measurements. Goodrich et al. (2011) specified the approach using piecewise linear fits for single ebullition events. However, the static threshold to determine ebullition events, as well as low-resolution measurements, limited the approach on estimating ebullition events which were characterized by a sudden concentration increase of ≥ 8 nmol mol^{-1} s^{-1}. This prevents a complete and clear flux separation. Moreover, CH$_4$ flux separation approaches based on manual chamber measurements with rather low temporal resolution fail to capture the rapidly changing absolute and relative contributions of the pathway-associated flux components both in time and space (Maeck et al., 2014; Walter et al., 2006).

Hence, there is a need for a non-intrusive method for separating pathway-associated CH$_4$ flux components. Improvements in measurement techniques, particularly by using high-resolution gas analysers (e.g. eddy covariance (EC) measurements), allow for high-temporal-resolution records of CH$_4$ emissions (Schrier-Uijl et al., 2011; Wille et al., 2008). Recently, a growing number of experimental GHG studies have employed automatic chambers (ACs) (Koskinen et al., 2014; Lai et al., 2014; Ramos et al., 2006), which can

provide flux data with an enhanced temporal resolution and capture short-term temporal (e.g. diurnal) dynamics. In addition, AC measurements can also represent small-scale spatial variability, and thus identify potential hot spots of CH$_4$ emissions (Koskinen et al., 2014; Lai et al., 2014). AC systems therefore combine the advantages of chamber measurements and micrometeorological methods with respect to the quantification of spatial as well as temporal dynamics of CH$_4$ emissions (Savage et al., 2014; Lai et al., 2012).

Combined with a high-resolution gas analyser (e.g. cavity ring-down spectroscopy), AC measurements provide opportunities for (i) detecting even minor ebullition events, and (ii) developing a statistically based flux separation approach. This study presents a new calculation algorithm for separating open-water CH$_4$ fluxes into its ebullition- and diffusion-derived components based on ebullition-related sudden concentration changes during chamber closure. A variable ebullition filter is applied using the lower and upper quartile and the interquartile range (IQR) of measured concentration changes. Data processing is based on the R script developed by Hoffmann et al. (2015). The script was modified for the purpose of CH$_4$ flux calculation and separation, thus including the advantages of automated and standardized flux estimation. We hypothesize that the presented flux calculation and separation algorithm together with the presented AC system can reveal concealed spatial and temporal dynamics in ebullition- and diffusion-associated CH$_4$ fluxes. This will facilitate the identification of relevant environmental drivers.

2 Material and methods

2.1 Automatic chamber system

In April 2013, an exemplary measurement site was equipped with an AC system and a nearby climate station (Fig. 1). The AC system consists of four rectangular transparent chambers, installed along a transect from the shoreline into the lake. Chambers are made of Lexan polycarbonate with a thickness of 2 mm and reinforced with an aluminium frame. Each chamber (volume of 1.5 m^3; base area 1 m^2) is mounted in a steel profile, secured by wires, and lifted/lowered by an electronically controlled cable winch located at the top of the steel profile. All chambers are equipped with a water sensor (capacitive limit switch KB 5004, efector150) at the bottom, which allows steady immersion (5 cm) of the chambers into the water surface. Hence, airtight sealing and constant chamber volume are ensured during the study period, despite possible changes of the water level. All chambers are connected by two tubes and a multiplexer to a single Los Gatos fast greenhouse gas analyser (911-0010, Los Gatos; gas flow rate: 5 L m^{-1}), which measures the air concentration of carbon dioxide (CO$_2$), methane (CH$_4$) and water vapour (H$_2$O). To ensure consistent air pressure and mixture during measurements, chambers are ventilated by a fan and
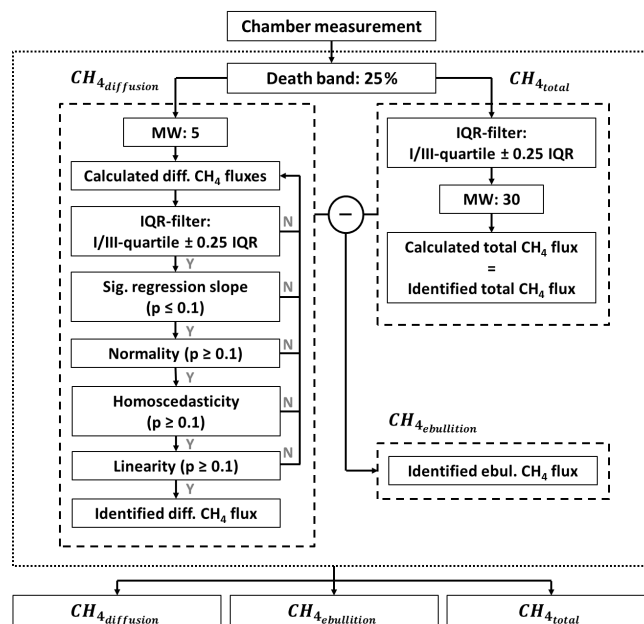
Figure 1. Transect of automatic chambers (ACs) established at the measurement site. The arrow indicates the position of the climate station near chamber II.

Figure 2. Flow chart showing the principles of the calculation of CH$_4$$_{\text{diffusion}}$ and CH$_4$$_{\text{total}}$ (dashed boxes) as well as subsequent CH$_4$ flux separation (dotted box).

sampled air is transferred back into the chamber headspace. However, due to the large chamber volume, mixture of the chamber headspace took up to 30 s. As a result of this, most peaks due to ebullition events were directly followed by a smaller decrease in measured CH$_4$ concentration. This indicates a short-term overestimation of the ebullition event (peak), which was compensated after the chamber headspace was mixed properly (decrease). This signal in the observed data is hereafter referred to as overcompensation. Concentration measurements are performed in sequence, sampling each chamber for 10 min with a 15 s frequency once per hour. When switching from one chamber to another, the tubes were vented for 2 min using the air of the open chamber to be measured next. Between two measurements at the same chamber position, each chamber was vented using the internal fan throughout the entire 50 min. A wooden boardwalk north of the measurement site allows for maintenance access, while avoiding disturbances of the water body and peat surface.

2.2 Flux calculation and separation algorithm

CH$_4$ flux calculation and separation was performed based on an adaptation of a standardized R script (Hoffmann et al., 2015). Figure 2 shows a flow chart of the flux calculation algorithm and the principle of the performed CH$_4$ flux separation. To estimate the relative contribution of diffusion and ebullition to total CH$_4$ emissions, flux calculation was performed twice (Fig. 3), once for the total CH$_4$ flux (CH$_4$$_{\text{total}}$) and once for the diffusive component of CH$_4$$_{\text{total}}$ (CH$_4$$_{\text{diffusion}}$), by adjusting selected user-defined parameter setups of the used R script. First of all, a death band of 25 % (user defined) was applied to the beginning of each flux measurement, thus excluding measurement artefacts triggered by the process of closing the chamber. On the remaining flux measurement data sets a variable moving window (MW) with a minimum

size of 5 (CH$_4$$_{\text{diffusion}}$; user defined) and 30 consecutive data points (CH$_4$$_{\text{total}}$; user defined) was applied. This generated several data subsets per flux measurement for CH$_4$$_{\text{diffusion}}$ and one data subset for CH$_4$$_{\text{total}}$. Subsequently, CH$_4$ fluxes were calculated for all data subsets per flux measurement using Eq. (1), where M is the molar mass of CH$_4$, A and V denote the basal area and chamber volume, respectively, and T and P represent the inside air temperature and air pressure. R is a constant (8.3143 m^3 Pa K^{-1} mol^{-1}).

$$r_{\text{CH}_4} \left(\mu\text{g C m}^{-2}\text{s}^{-1} \right) = \frac{M \times P \times V \times \delta v}{R \times T \times t \times A} \tag{1}$$

In the case of CH$_4$$_{\text{total}}$, δv is calculated as the difference between the start and end CH$_4$ concentration of the enlarged MW (30 consecutive data points; 7.5 min). To avoid measurement artefacts (e.g. overcompensation), being taken into account as start or end concentration, measurement points representing an inherent concentration change smaller or larger than the upper and lower quartile ± 0.25 times IQR (user defined) were discarded prior to calculation of CH$_4$$_{\text{total}}$. In the case of diffusion, δv is the slope of a linear regression fitted to each data subset. The resulting numerous CH$_4$$_{\text{diffusion}}$ fluxes calculated per measurement (based on the moving window data subsets) were further evaluated according to different exclusion criteria: (i) range of within-chamber air temperature not larger than ± 1.5 K; (ii) significant regression slope ($p \leq 0.1$); and (iii) non-significant tests ($p > 0.1$) for normality (Lilliefors' adaption of the Kolmogorov–Smirnov test), homoscedasticity (Breusch–Pagan test) and linearity. In addition (iv) abrupt concentration changes within each
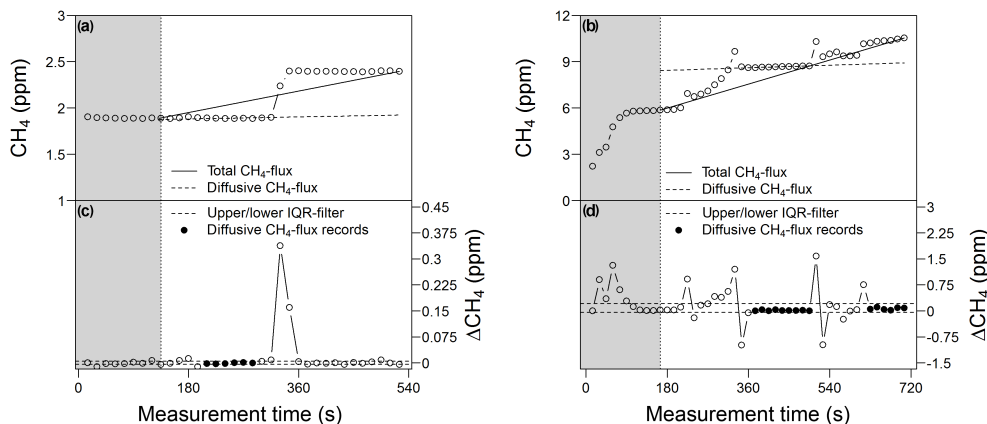
Figure 3. Time series plot of recorded concentrations (ppm) within the chamber headspace for **(a)** a simulated ebullition event and **(b)** an exemplary field study CH$_4$ measurement. Time spans dominated by diffusive CH$_4$ release are marked by **(c, d)** black dots, enclosed by the 25 and 75 % quantiles ± 0.25 IQR of obtained concentration changes, shown as black dashed lines. Unfilled dots outside the dashed lines display ebullition events (see also Goodrich et al., 2011; Miller and Oremland, 1988). Grey shaded areas indicate the applied death band at the beginning of each measurement (25 %). Negative ΔCH$_4$ values indicate a overcompensation due to (temporally) insufficient headspace mixing.

MW data subset were identified by a rigid outlier test, which discarded fluxes with an inherent concentration change outside of the range between the upper and lower quartile ± 0.25 times (user defined) the interquartile range (IQR). Calculated CH$_{4_{\text{diffusion}}}$ fluxes which did not meet all exclusion criteria were discarded. In the case of more than one flux per measurement meeting all exclusion criteria, the CH$_{4_{\text{diffusion}}}$ flux with a starting CH$_4$ concentration being closest to the atmospheric CH$_4$ concentration was chosen. Finally, the proportion of the total CH$_4$ emission released via ebullition was estimated by subtracting identified CH$_{4_{\text{diffusion}}}$ from the calculated CH$_{4_{\text{total}}}$ following Eq. (2).

$$CH_{4_{\text{ebullition}_n}} = \sum_{i=1}^{n} \left(CH_{4_{\text{total}}} - CH_{4_{\text{diffusion}}} \right) \qquad (2)$$

Since no emergent macrophytes were present below the automatic chambers, plant-mediated transport of CH$_4$ was assumed to be zero. The same accounts for negative estimates of CH$_4$ released through ebullition. The used R script, a manual and test data set are available at https://zenodo.org/record/53168.

2.3　Verification of applied flux separation algorithm

A laboratory experiment was performed under controlled conditions to verify the used flux separation algorithm. In order to artificially simulate ebullition events, distinct amounts (5, 10, 20, 30 and 50 mL) of a gaseous mixture (25 000 ppm CH$_4$ in artificial air; Linde, Germany) were inserted by a syringe through a pipe into a water-filled tub (12 L) covered with a closed chamber (headspace $V = 0.114\,\text{m}^3$; $A = 0.145\,\text{m}^2$). The water within the tub was not replaced during the laboratory experiment, thus ensuring CH$_4$ saturation after

the first simulations of ebullition events. Airtight sealing was achieved by a water-filled frame, connecting tub and chamber. The chamber was ventilated by a fan and connected via pipes to a Los Gatos greenhouse gas analyser (911-0010, Los Gatos), measuring CH$_4$ concentrations inside the chamber with a 1 Hz frequency (Fig. 4). To ensure comparability between in vitro and in situ measurements, data processing was performed based on 0.066 Hz records. The expected concentration changes within the chamber headspace as the result of injected CH$_4$ were calculated as the mixing ratio between the amount of inserted gaseous mixture (25 000 ppm) and the air-filled chamber volume (2 ppm).

2.4　Exemplary field study

Ecosystem CH$_4$ exchange was measured from beginning of July to end of September 2013 at a flooded former fen grassland site, located within the Peene river valley in Mecklenburg-West Pomerania, northeast Germany (53°52′ N, 12°52′ E). The long-term annual precipitation is 570 mm. The mean annual air temperature is 8.7 °C (DWD, Anklam). The study site was particularly influenced by a complex melioration and drainage programme between 1960 and 1990, characterized by intensive agriculture. As a consequence, the peat layer was degraded and the soil surface was lowered by subsidence. Being included in the Mecklenburg-West Pomerania mire restoration programme, the study site was rewetted in the beginning of 2005. As a result, the water level rose above the soil surface, thus transforming the site into a shallow lake. Exceptionally high CH$_4$ emissions at the measurement site were reported by Franz et al. (2016), who measured CO$_2$ and CH$_4$ emissions using an eddy covariance system, and Hahn-Schöffl et al. (2011), who investigated sed-
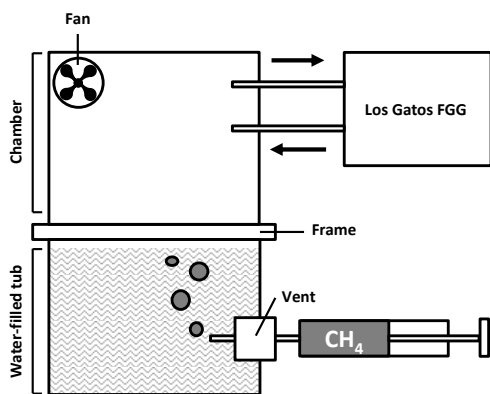
Figure 4. Scheme of experimental setup used for the simulation and determination of ebullition events with a Los Gatos fast greenhouse gas (FGG) analyser (911-0010, Los Gatos). The crimped area represents water-filled tub.

Figure 5. Scatter plot of the amount of injected CH_4 and the corresponding calculated CH_4 ebullition event. The solid black line indicates the 1 : 1 agreement. The linear fit between the displayed values is represented by the black dashed line, surrounded by the 95 % confidence interval (grey shaded area).
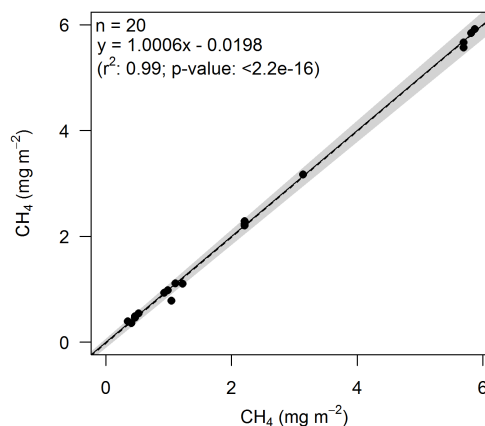
iments formed during inundation. Prior to rewetting, the vegetation was dominated by reed canary grass (*Phalaris arundinacea*), which disappeared after rewetting due to permanent inundation. At present, the water surface is partially covered with duckweed (Lemnoideae), while broadleaf cattail (*Typha latifolia*) and reed mannagrass (*Glyceria maxima*) are present next to the shoreline (Franz et al., 2016; Hahn-Schöffl et al., 2011). However, below the chambers, no emergent macrophytes were present throughout the study period.

Temperatures were recorded in the water (5 cm above sediment surface) and different sediment depths (2, 5 and 10 cm below the sediment–water interface), using thermocouples (T107, Campbell Scientific). Additionally, air temperature at 20 and 200 cm height, wind speed, wind direction, precipitation, relative humidity and air pressure were measured by a nearby climate station (WXT52C, Vaisala). Water table depth was measured by a pressure probe (PDCR1830, Campbell Scientific). All parameters were continuously recorded at 30 min intervals and stored by a data logger (CR 1000, Campbell Scientific) connected to a GPRS radio modem.

3 Results and discussion

3.1 Verification of the flux separation algorithm

A good overall agreement was found during the laboratory experiment between $CH_{4_{ebullition}}$ fluxes calculated for the simulated ebullition events and the amount of injected CH_4. This supports the assumption of using sudden changes in chamber-based CH_4 concentration measurements to separate diffusion and ebullition flux components and shows the accuracy of the presented algorithm (Fig. 5). However, when applied under field conditions, flux separation might be biased due to a steady flux originating from other processes than diffusion through peat and water layers, such as the steady ebullition of microbubbles (Prairie and del Giorgio,

2013; Goodrich et al., 2011). To minimize the potential impact of the steady ebullition of microbubbles on calculated $CH_{4_{diffusion}}$, the concentration measurement frequency during chamber closure should be enhanced. This allows identifying and filtering small-scale differences within measured concentration changes using the variable IQR criterion, which thereby reduces the detection limit of ebullition events.

3.2 Application to an exemplary field study

Time series of measured $CH_{4_{total}}$ fluxes, integrated over the four chambers of the transect, as well as the respective contributions of ebullition and diffusion, are shown in Fig. 6. Apart from short-term measurement gaps, a considerable loss of data occurred between 27 July and 7 August 2013 due to malfunction of the measurement equipment. $CH_{4_{total}}$ fluxes observed by the AC system and calculated with the presented algorithm were comparable to CH_4 emissions measured during the study period by a nearby eddy covariance system (Franz et al., 2016). This indicates the general accuracy of the used measurement system and calculation algorithm.

Observed $CH_{4_{total}}$ fluxes showed distinct seasonal patterns following the temperature regime at 10 cm sediment depth. This is in accordance with Christensen et al. (2005) and Bastviken et al. (2004), who showed that biochemical processes driving CH_4 production are closely related to temperature regimes, determining the CH_4 production within the sediment. In addition to seasonality, $CH_{4_{total}}$ also featured diurnal dynamics, with lower fluxes during daytime and higher fluxes during nighttime, which were most pronounced during July and early September (Fig. 6). During August, the diurnal variability was superimposed by short-term emission events and high amplitudes in recorded $CH_{4_{total}}$. Similar to $CH_{4_{total}}$, diffusive fluxes also showed a
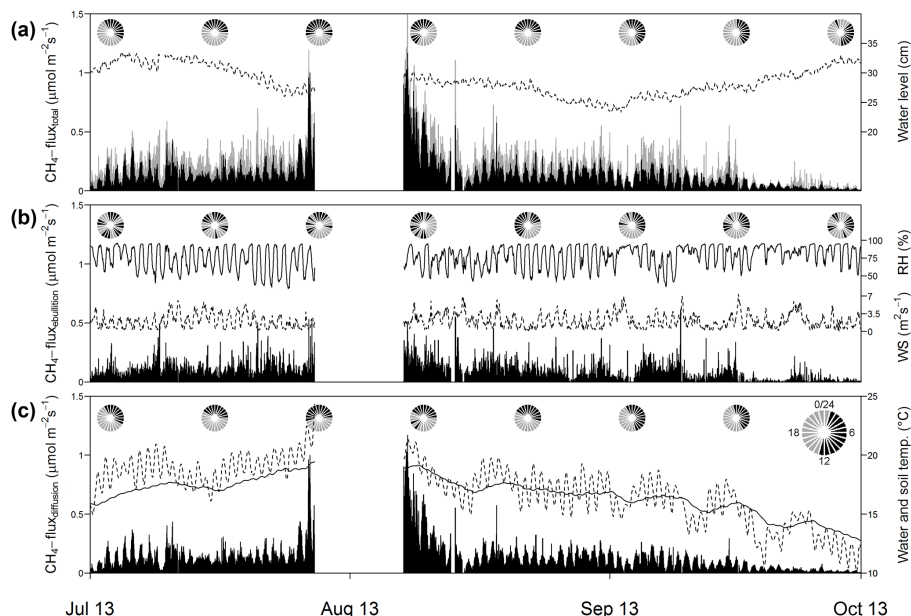
Figure 6. Time series of **(a)** total CH$_4$ emissions with proportions of ebullition (grey bar) and diffusion flux components (black bar) during the study period from July until September 2013. Figure 6b and c show the separated flux components (**b** ebullition and **c** diffusion), together with the development of important environmental parameters, which are assumed to explain their specific dynamics (**a** water level, **b** RH and wind speed and **c** sediment (solid line) and water temperature (dashed line)). Pie charts represent the biweekly pooled diurnal cycle of measured CH$_4$ fluxes. Slices are applied clockwise, creating a 24 h clock, with black and light grey slices indicating hours with CH$_4$ flux above and below the daily mean, respectively.

distinct temperature-driven seasonality as well as clear diurnal patterns throughout the entire study period (Fig. 7). However, compared to the diurnal variability of CH$_{4\mathrm{total}}$ fluxes, a pronounced shift of maximum emissions from early morning to nighttime hours was revealed for CH$_{4\mathrm{diffusion}}$ during August 2013 (Figs. 6, 7). While maximum CH$_{4\mathrm{diffusion}}$ fluxes during July were recorded during early morning hours (approx. 03:00 to 06:00 CET), a shift to the nighttime was observed for August (max. from 21:00 to 00:00 CET). During September maximum fluxes shifted back to the early morning, with maximum fluxes between 00:00 and 09:00 CET (Fig. 6). This could be explained by differences in turbulent mixing due to changing water temperature gradients. During daytime, the surface water is warmed, thus preventing an exchange with the CH$_4$-enriched water near the sediment, which results in lower fluxes for CH$_{4\mathrm{diffusion}}$. During nighttime, when the upper water layer cools down and mixing is undisturbed, enhanced CH$_{4\mathrm{diffusion}}$ fluxes can be detected. These dynamics are more pronounced during warm days, explaining the seasonal shift, and concealed during periods with a high wind velocity. The obtained diurnal trend is in accordance with findings of Sahlée et al. (2014) and Lai et al. (2012), who reported higher nighttime and lower daytime CH$_4$ emissions for a lake site in Sweden and an ombrotrophic bog in Canada, respectively. However, an opposing tendency was found by Deshmukh et al. (2014), who reported higher daytime and lower nighttime CH$_4$ emissions

from a newly flooded subtropical freshwater hydroelectric reservoir within the Nam Theun river valley, Laos. In contrast to diurnal trends obtained for CH$_{4\mathrm{total}}$ and CH$_{4\mathrm{diffusion}}$, estimated ebullition events occurred erratically and showed neither clear seasonal nor diurnal dynamics. Nonetheless, periods characterized by more pronounced ebullition seemed to roughly follow the sediment temperature-driven CH$_4$ production within the sediment as, for example, reported by Bastviken et al. (2004) (Fig. 5). This is confirmed by a distinct correlation between daily mean sediment temperatures and corresponding sums of measured ebullition fluxes (r^2: 2 cm = 0.63; 5 cm = 0.63; 10 cm = 0.62). Moreover, fewer and smaller ebullition events were detected in times of reduced wind velocity and high relative humidity (RH) (e.g. 10–11 September and 18–19 September 2013). However, at the level of single flux measurements, no significant dependency was found between the recorded environmental drivers and CH$_4$ release via ebullition. The relative contributions of diffusion and ebullition were 55 % (min. 33 to max. 70 %) and 46 % (min. 30 to max. 67 %), respectively. This is in accordance with values reported by Bastviken et al. (2011), who compiled CH$_4$ emission estimates from 474 freshwater ecosystems with clearly defined emission pathways. A similar ratio was also found by Tokida et al. (2007), who investigated the role of decreasing atmospheric pressure as a trigger for CH$_4$ ebullition events in peatlands.
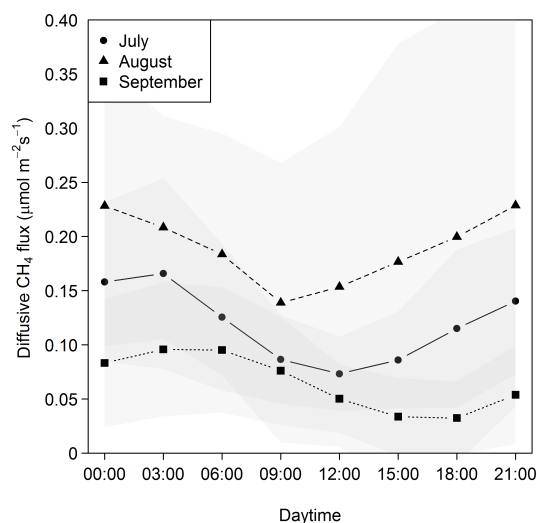
Figure 7. Monthly averaged diurnal cycle of diffusive CH$_4$ fluxes indicating differences in magnitude and amplitude as well as a shift in minimum and maximum daily CH$_4$ fluxes over the course of the study period.

Comparison of flux data among the four chambers reveals considerable spatial heterogeneity within the measured transect (data not shown). Monthly averages of diffusive, ebullition and total CH$_4$ emissions for all four chambers of the established transect as well as statistics showing the explanatory power of different environmental variables are summarized in Table 1. With respect to total CH$_4$ emissions, neighbouring chambers generally featured high differences in CH$_4$ fluxes, with no obvious trend along the transect. The same holds true for derived ebullition and diffusive CH$_4$ flux components. After separation into diffusion and ebullition, flux-component-specific dependencies on different environmental drivers were revealed (Table 1).

3.3 Overall performance

Compared to direct measurements of diffusion or ebullition (e.g. Bastviken et al., 2010, 2004) the presented calculation algorithm features two major advantages. On the one hand it allows deriving ebullition and diffusion flux components based on the same measurement and spatial entity, which prevents an interfering influence of spatial heterogeneity on observed flux components. This is not the case for flux separation based on a combination of different measurement devices, such as automatic chambers and bubble traps, which need a sufficient number of repetitions and degree in data aggregation to reduce the bias, emerging from the spatiotemporal heterogeneity of erratically occurring ebullition events. On the other hand, the solely data-processing-based flux separations approach allows for an application when the use of direct measurement systems for either ebullition (gas traps, funnels) or diffusion (bubble shields) might be limited. This

Table 1. Monthly averages ± 1 standard deviation of hourly CH$_4$ emissions (mg m^{-2} h^{-1}) for the chamber transect (from chamber I–IV, starting near the shoreline). Average standardized (beta) coefficients and Nash–Sutcliffe efficiency (NSE) based on linear regressions and multiple linear regressions between different environmental drivers and daily subsets of calculated CH$_4$ emissions are shown below. Monthly averages as well as statistics are separated according to diffusion, ebullition and total CH$_4$ flux. Superscript letters indicate significant differences between chambers and the p values of applied linear and multiple linear regressions (MLRs).

Month	Chamber	CH$_4$$_{\text{diffusion}}$	CH$_4$$_{\text{ebullition}}$	CH$_4$$_{\text{total}}$
		mg m^{-2} h^{-1}		
July	I	4.6$^{\text{bd}}$ $\pm$ 3.1	5.5 $\pm$ 7.0	10.1$^{\text{bd}}$ $\pm$ 7.8
	II	1.8$^{\text{acd}}$ $\pm$ 1.5	3.7 $\pm$ 6.9	5.5$^{\text{acd}}$ $\pm$ 7.1
	III	6.1$^{\text{bd}}$ $\pm$ 4.0	4.7 $\pm$ 6.9	10.7$^{\text{bd}}$ $\pm$ 8.2
	IV	8.7$^{\text{abc}}$ $\pm$ 5.9	4.7 $\pm$ 5.3	13.3$^{\text{abc}}$ $\pm$ 7.6
August	I	5.1 $\pm$ 5.9	5.0$^{\text{bd}}$ $\pm$ 6.8	10.1 $\pm$ 10.0
	II	3.7 $\pm$ 5.0	2.9$^{\text{ad}}$ $\pm$ 6.0	6.5 $\pm$ 8.6
	III	5.7 $\pm$ 4.9	5.8$^{\text{bd}}$ $\pm$ 7.4	11.5 $\pm$ 9.5
	IV	6.1 $\pm$ 6.8	3.0$^{\text{ac}}$ $\pm$ 5.0	9.1 $\pm$ 9.4
September	I	2.3$^{\text{bd}}$ $\pm$ 2.0	1.8$^{\text{bd}}$ $\pm$ 3.9	4.1$^{\text{bd}}$ $\pm$ 4.8
	II	2.6$^{\text{a}}$ $\pm$ 2.7	1.1$^{\text{ac}}$ $\pm$ 3.0	3.7$^{\text{ac}}$ $\pm$ 4.4
	III	3.9$^{\text{d}}$ $\pm$ 3.9	5.4$^{\text{bd}}$ $\pm$ 6.9	9.3$^{\text{bd}}$ $\pm$ 8.8
	IV	1.3$^{\text{ac}}$ $\pm$ 1.6	0.7$^{\text{ac}}$ $\pm$ 3.4	2.1$^{\text{ac}}$ $\pm$ 4.0
Mean		5.1 $\pm$ 5.7	4.2 $\pm$ 6.5	9.2 $\pm$ 9.6

Driver	CH$_4$$_{\text{diffusion}}$	CH$_4$$_{\text{ebullition}}$	CH$_4$$_{\text{total}}$
	Average standardized (beta) coefficient of daily data subsets		
wind velocity	-0.4^{e}	-0.1	-0.3^{e}
relative humidity (RH)	0.5$^{\text{f}}$	0.1	0.4$^{\text{e}}$
air pressure	0.0	-0.1	0.0
water level	-0.5^{f}	-0.1	-0.4^{e}
air temperature (2 m)	-0.6^{f}	-0.1	-0.4^{e}
water temperature (5 cm)	0.1$^{\text{e}}$	0.1	0.1$^{\text{e}}$
sediment temperature (2 cm)	0.3$^{\text{e}}$	0.0	0.2$^{\text{e}}$
Δ water-air temperature	0.6$^{\text{f}}$	0.1	0.4$^{\text{e}}$
average NSE of MLR	0.72	0.30	0.51

Significant difference (Tukey HSD test; $\alpha \leq 0.1$) between [a] chamber I, [b] II, [c] III and [d] IV. Significant dependency with average [e] p value < 0.2 and [f] p value < 0.1.

is in particular the case when measuring at wetland ecosystem with a varying water level, such as at the exemplary study site (22 to 35 cm). During the summer months of 2009 and 2016 the water level dropped substantially, being either next to or even below the surface (data not shown). This limited a potential application of bubble traps and shields to periods with a sufficient water level, despite ebullition from the water-saturated sediment during periods with low water level. In addition to that, the AC system and presented flux separation algorithm allows for parallel measurements of different trace gases (e.g. CO$_2$ and CH$_4$) at the same chamber position.

However, flux separation using the presented algorithm might be biased by steady ebullition of microbubbles and frequently occurring strong ebullition events. Steady ebullition

of microbubbles results in an overestimation of CH$_{4_{\text{diffusion}}}$ and underestimation of CH$_{4_{\text{ebullition}}}$, an effect that might be reduced by enhancing the measurement frequency and thus the sensitivity of the variable IQR filter. Compared to that, frequently occurring strong ebullition events might disable the calculation of CH$_{4_{\text{diffusion}}}$, which hampers flux separation for the corresponding measurement. Out of 14 828 valid automatic chamber measurements during the exemplary field study, the algorithm failed to calculate CH$_{4_{\text{diffusion}}}$ during 170 measurements. This equals 1.15 % of all measurements. Taking into account that the presented measurement site is characterized by rather large CH$_4$ emissions (Franz et al., 2016) and frequently occurring ebullition events (Fig. 3), this limitation seems to be negligible.

Compared to other data-processing-based approaches for CH$_4$ flux separation (e.g. Goodrich et al., 2011; Miller and Oremland, 1988), the presented algorithm calculates an integrated ebullition flux component. This ensures a reliable flux separation, despite potential measurement artefacts such as overcompensation or incomplete ebullition records.

Accounting for the few prerequisites (high-resolution closed chamber measurements) as well as mentioned advantages, an application of the presented approach to open-water areas of a broad range of wetland ecosystems and automatic closed chamber systems is stated.

4 Conclusions

The results of the laboratory experiment as well as the estimated relative contributions of ebullition and diffusion during the field study indicate that the presented algorithm for CH$_4$ flux calculation and separation into diffusion and ebullition delivers reasonable and robust results. Temporal dynamics, spatial patterns and relations to environmental parameters well established in the scientific literature, such as sediment temperature, water temperature gradients and wind velocity, became more pronounced when analysed separately for diffusive CH$_4$ emissions and ebullition. The presented algorithm will be applicable as long as the underlying closed chamber measurements deliver continuous high-resolution records of CH$_4$ concentrations and air temperature. However, steady ebullition of microbubbles might yield an overestimation of the diffusive flux component, whereas continuously strong ebullition events might totally prevent flux separation. Hence, the application and adaptation of the presented algorithm for different wetland ecosystems and automatic chamber designs is needed. Obtained results should be further validated against direct flux measurements using, for example, bubble traps or barriers. This will allow evaluating the generalizability and applicability to other freshwater and wetland ecosystems as well as chamber designs.

Despite the mentioned shortcomings, the presented calculation algorithm for separating CH$_4$ emissions increases the amount of information about the periodicity of CH$_4$ release

and may help to reveal the influence of potential drivers as well as to explain temporal and spatial variability within both separated flux components. In future, the implementation of CH$_4$ released through plant-mediated transport into the flux separation algorithm should be addressed. This could be realized by complete chamber measurements with CH$_4$ concentrations measured in different water and/or sediment depth, which will allow the direct derivation of CH$_{4_{\text{diffusion}}}$. In a next step, the remaining two flux components could be separated using the presented algorithm.

5 Data availability

The presented simple calculation algorithm, a test data set and manual, as well as all raw data sets of automatic chamber flux measurements shown in this study, are available at https://zenodo.org (Hoffmann and Jurisch, 2016; Hoffmann et al., 2017).

References

Bastviken, D., Cole, J. J., Pace, M. L., and Tranvik, L. J.: Methane emissions from lakes: Dependence of lake characteristics, two regional assessments, and a global estimate, Global Biogeochem. Cy., 18, GB4009, doi:10.1029/2004GB002238, 2004.

Bastviken, D., Santoro, A. L., Marotta, H., Queiroz Pinho, L., Fernandes Calheiros, D., Crill, P., and Enrich-Prast, E.: Methane Emissions from Pantanal, South America, during the low water season: towards more comprehensive sampling, Environ. Sci. Technol., 44, 5450–5455, 2010.

Bastviken, D., Tranvik, L. J., Downing, J. A., Crill, P. M., and Enrich-Prast, A.: Freshwater methane emissions offset the continental carbon sink, Science, 331, 50, doi:10.1126/science.1196808, 2011.

Chanton, J. P. and Whiting, G. J.: Trace gas exchange in freshwater and coastel marine environments: ebullition and transport by plants, in: Biogenic trace gases: measuring emissions from soil and water, chap. 4, edited by: Matson, P. A. and Hariss, R. C., Blackwell Science Ltd., UK, 98–125, 1995.

Christensen, T. R., Ekberg, A., Ström, L., Mastepanov, M., and Panikov, N.: Factors controlling large scale variations in methane emissions from wetlands, Geophys. Res. Lett., 30, 1414, doi:10.1029/2002GL016848, 2005.

DelSontro, T., Kunz, M. J., Kempter, T., Wüest, A., Wehrli, B., and Senn, D. B.: Spatial heterogeneity of methane ebullition in a large tropical reservoir, Environ. Sci. Technol., 45, 9866–9873, 2011.

Dengel, S., Zona, D., Sachs, T., Aurela, M., Jammet, M., Parmentier, F. J. W., Oechel, W., and Vesala, T.: Testing the applicability of neural networks as a gap-filling method using CH$_4$ flux data from high latitude wetlands, Biogeosciences, 10, 8185–8200, doi:10.5194/bg-10-8185-2013, 2013.

Deshmukh, C., Serça, D., Delon, C., Tardif, R., Demarty, M., Jarnot, C., Meyerfeld, Y., Chanudet, V., Guédant, P., Rode, W., Descloux, S., and Guérin, F.: Physical controls on CH$_4$ emissions from a newly flooded subtropical freshwater hydroelectric reservoir: Nam Theun 2, Biogeosciences, 11, 4251–4269, doi:10.5194/bg-11-4251-2014, 2014.

Franz, D., Koebsch, F., Larmanou, E., Augustin, J., and Sachs, T.: High net CO$_2$ and CH$_4$ release at a eutrophic shallow lake on a formerly drained fen, Biogeosciences, 13, 3051–3070, doi:10.5194/bg-13-3051-2016, 2016.

Goodrich, J. P., Varner, R. K., Frolking, S., Duncan, B. N., and Crill, P. M.: High-Frequency measurements of methane ebullition over a growing season at a temperate peatland site, Geophys. Res. Lett., 38, L07404, doi:10.1029/2011GL046915, 2011.

Hahn-Schöfl, M., Zak, D., Minke, M., Gelbrecht, J., Augustin, J., and Freibauer, A.: Organic sediment formed during inundation of a degraded fen grassland emits large fluxes of CH$_4$ and CO$_2$, Biogeosciences, 8, 1539–1550, doi:10.5194/bg-8-1539-2011, 2011.

Hoffmann, M. and Jurisch, N.: A simple calculation algorithm to separate high-resolution CH$_4$ flux measurements into ebullition- and diffusion-derived components, doi:10.5281/zenodo.53168, 2016.

Hoffmann, M., Jurisch, N., Albiac Borraz, E., Hagemann, U., Drösler, M., Sommer, M., and Augustin, J.: Automated modeling of ecosystem CO$_2$ fluxes based on periodic closed chamber measurements: A standardized conceptual and practical approach, Agr. Forest Meteorol., 200, 30–45, 2015.

Hoffmann, M., Schulz-Hanke, M., Garcia Alba, J., Jurisch, N., Hagemann, U., Sachs, T., Sommer, M., and Augustin, J.: Data sets for: A simple calculation algorithm to separate high-resolution CH$_4$ flux measurements into ebullition- and diffusion-derived components (AMT), doi:10.5281/zenodo.229138, 2017.

Huttunen, J. T., Lappalainen, K. M., Saarijärvi, E., Väisänen, T., and Martikainen, P. J.: A novel sediment gas sampler and a sibsurface gas collector used for measurment of the ebullition of methane and carbon dioxide from a eutrophied lake, Sci. Total Environ., 266, 153–158, 2001.

IPCC: Summary for Policymakers, in: Climate Change 2013, The Physical Science Basis, Working Group I Contribution to the Fifth Assessment Report of the Intergovernmental Panel on Climate Change, edited by: Stocker, T. F., Qin, D., Plattner, G.-K., Tignor, M. M. B., Allen, S. K., Boschung, J., Nauels, A., Xia, Y., Bex, V., and Midgley, P. M., Cambridge University Press, Cambridge, UK and New York, NY, USA, 2013.

Koch, S., Jurasinski, G., Koebsch, F., Koch, M., and Glatzel, S.: Spatial variability of annual estimates of methane emissions in a Phragmites Australis (Cav.) Trin. Ex Steud. dominated restored brakish fen, Wetlands, 34, 593–602, 2014.

Koebsch, F., Jurasinski, G., Koch, M., Hofmann, J., and Glatzel, S.: Controls for multi-scale temporal variation in ecosystem methane exchange during the growing season of a permanently inudated fen, Agr. Forest Meteorol., 204, 94–105, 2015.

Koskinen, M., Minkkinen, K., Ojanen, P., Kämäräinen, M., Laurila, T., and Lohila, A.: Measurements of CO$_2$ exchange with an automated chamber system throughout the year: challenges in measuring night-time respiration on porous peat soil, Biogeosciences, 11, 347–363, doi:10.5194/bg-11-347-2014, 2014.

Lai, D. Y. F., Roulet, N. T., Humphreys, E. R., Moore, T. R., and Dalva, M.: The effect of atmospheric turbulence and chamber deployment period on autochamber CO$_2$ and CH$_4$ flux measurements in an ombrotrophic peatland, Biogeosciences, 9, 3305–3322, doi:10.5194/bg-9-3305-2012, 2012.

Lai, D. Y. F., Roulet, N. T., and Moore, T. R.: The spatial and temporal relationship between CO$_2$ and CH$_4$ exchange in a temperate ombrotropic bog, Atmos. Environ., 89, 249–259, 2014.

Limpens, J., Berendse, F., Blodau, C., Canadell, J. G., Freeman, C., Holden, J., Roulet, N., Rydin, H., and Schaepman-Strub, G.: Peatlands and the carbon cycle: from local processes to global implications – a synthesis, Biogeosciences, 5, 1475–1491, doi:10.5194/bg-5-1475-2008, 2008.

Maeck, A., Hofmann, H., and Lorke, A.: Pumping methane out of aquatic sediments – ebullition forcing mechanisms in an impounded river, Biogeosciences, 11, 2925–2938, doi:10.5194/bg-11-2925-2014, 2014.

Miller, L. G. and Oremland, R. S.: Methane efflux from the pelagic regions of four lakes, Global Biogeochem. Cy., 2, 269–277, 1988.

Ostrovsky, I., McGinnis, D. F., Lapidus, L., and Eckert, W.: Quantifying gas ebullition with echo sounder: the role of methane transport by bubbles in a medium-sized lake, Limnol. Oceanogr.-Meth., 6, 105–118, 2008.

Prairie, Y. T. and del Giorgio, P. A.: A new pathway of freshwater methane emissions and the putative importance of microbubbles, Inland Waters, 3, 311–320, 2013.

Ramos, F. M., Lima, I. B. T., Rosa, R.R., Mazzi, E. A., Carvalho, J. C., Rasera, M. F. F. L., Ometto, J. P. H. B., Assireu, A. T., and Stech, J. L.: Extreme event dynamics in methane ebullition fluxes from tropical reservoirs, Geophys. Res. Lett., 33, L21404, doi:10.1029/2006GL027943, 2006.

Repo, M. E., Huttunen, J. T., Naumov, A. V., Chichulin, A. V., Lapshina, E. D., Bleuten, W., and Martikainen, P. J.: Release of CO$_2$ and CH$_4$ from small wetland lakes in western Siberia, Tellus B, 59, 788–796, 2007.

Sahlée, E., Rutgersson, A., Podgrajsek, E., and Bergström, H.: Influence from surrounding Land on the turbulence measurments above a lake, Bound.-Lay. Meteorol., 150, 235–258, 2014.

Savage, K., Phillips, R., and Davidson, E.: High temporal frequency measurements of greenhouse gas emissions from soils, Biogeosciences, 11, 2709–2720, doi:10.5194/bg-11-2709-2014, 2014.

Schrier-Uijl, A. P., Veraart, A. J., Leffelaar, P. A., Berendse, F., and Veenendaal, E. M.: Release of CO$_2$ and CH$_4$ from lakes and drainage ditches in temperate wetlands, Biogeochemistry, 102, 265–279, 2011.

Tokida, T., Miyazaki, T., Mizoguchi, M., Nagata, O., Takakai, F., Kagemoto, A., and Hatano, R.: Falling atmospheric pressure as a trigger for methane ebullition from peatland, Global Biogeochem. Cy., 21, GB2003, doi:10.1029/2006GB002790, 2007.

Van der Nat, F. W. and Middelburg, J.: Methane emission from tidal freshwater marshes, Biogeochemistry, 49, 103–121, 2000.

Walter, K. M., Zimov, S. A., Chanton, J. P., Verbyla, D., and Chapin III, F. S.: Methane bubbling from siberian thaw lakes as a positive feedback to climate warming, Nature, 443, 71–75, 2006.

Walter, K. M., Chanton, J. P., Chapin III, F. S., Schuur, E. A. G., and Zimov, S. A.: Methane production and bubble emissions from arctic lakes: Isotopic implications for source pathways and ages, J. Geophys. Res., 113, G00A08, doi:10.1029/2007JG000569, 2008.

Walter, K. M., Smith, L. C., and Chapin III, F. S.: Methane bubbling from northern lakes: present and future contributions to the global methane budget, Philos. T. Roy. Soc. A., 365, 1657–1676, 2015.

Whiting, G. J. and Chanton, J. P.: Control of the diurnal pattern of methane emission from emergent aquatic macrophytes by gas transport mechnaisms, Aquat. Bot., 54, 237–253, 1996.

Wik, M., Crill, P. M., Bastviken, D., Danielsson, A., and Norbäck, E.: Bubbles trapped in arctic lake ice: Potential implications for methane emissions, J. Geophys. Res., 116, G03044, doi:10.1029/2011JG001761, 2011.

Wik, M., Crill, P. M., Varner, R. K., and Bastviken, D.: Multiyear measurements of ebullitive methane fluy from three subarctic lakes, J. Geophys. Res.-Biogeo., 118, 1307–1321, 2013.

Wille, C., Kutzbach, L., Sachs, T., Wagner, D., and Pfeiffer, E.-M.: Methane emissions from Siberian artic polygonal tundra: eddy covariance measurements and modeling, Glob. Change Biol., 14, 1395–1408, 2008.

Yu, Z., Slater, L. D., Schafer, K. V. R., Reeve, A. S., and Varner, R. K.: Dynamics of methane ebullition from a peat monolith revealed from a dynamic flux chamber system, J. Geophys. Res.-Biogeo., 119, 1789–1806, 2014.